Elasto/Visco-Plastic Dynamic Response of Axisymmetrical Shells Under Mechanical and/or Thermal Loading*

Katsumi TAO**, Shigeo TAKEZONO**,
Toshihiro TAGUCHI** and Kazuo HOTADA***

An analytical method for the elasto/visco-plastic dynamic problems of axisymmetrical thin shells subjected to mechanical and/or thermal loads is developed. The equations of motion and the relations between the strains and displacements are derived by extending Sanders' elastic shell theory. For the constitutive relations, Perzyna's elasto/visco-plastic equations including the temperature effect are employed. The derived fundamental equations are numerically solved by the finite difference method. As numerical examples, the simply supported cylindrical shells made of mild steel are treated and the following two cases are analyzed: a nonuniform temperature cylinder subjected to impulsive internal pressure, and an internal pressure cylinder subjected to impulsive thermal load. In both cases the variations of displacements and internal forces with time are discussed.

Key Words: Structural Analysis, Thermal Stress, Finite Difference Method, Elasto/Visco-Plasticity, Dynamic Response, Shells

1. Introduction

Many investigations on the elasto/visco-plastic dynamic response of shells to time-dependent loads have been carried out not only for axisymmetrical shells but also for general asymmetrical shells[1]~[5]. These investigations, however, deal with cases maintaining a constant temperature distribution in the shell body. Only a few investigations on the problems for nonuniform temperature distribution have been performed[6],[7].

In the present paper, the authors study the elasto/visco-plastic dynamic response of axisymmetrical thin shells to general asymmetrical mechanical and/or thermal loads. The equations of motion derived from Sanders' theory for thin shells[8] by adding the inertia terms are used. As the constitutive relation, Hooke's law is used in the linear elastic range, and Perzyna's elasto/visco-plastic equations[9] including the temperature effect are employed in the plastic range. In the numerical analysis of the fundamental equations for incremental values an usual finite difference form is employed for the spatial derivatives and the inertia terms are treated with the backward difference formula proposed by Houbolt[10]. The solutions are obtained by integration of the incremental values.

As numerical examples, a nonuniformly heated cylindrical shell subjected to impulsive internal pressure and an internally pressurized cylindrical shell subjected to impulsive thermal load are analyzed.

2. Fundamental Equations

Let the undeformed middle surface of axisymmetrical shells be given by the orthogonal coordinate system (ξ, θ) and ζ be directed outward from the middle surface, as shown in Fig. 1, then the relations among the nondimensional curvatures $\omega_\xi(=a/R_s)$, $\omega_\theta(=a/R_\theta)$ and the nondimensional radius $\rho(=r/a)$ become as follows:

* Received 23rd January, 1989. Paper No. 87-1294 A
** Department of Energy Engineering, Toyohashi University of Technology, Tempaku-cho, Toyohashi, 440, Japan
*** TOTO Ltd., Kokurakita-ku, Kitakyushu, 802, Japan

$$\left.\begin{aligned}&\omega_\xi=-(\gamma'+\gamma^2)/\omega_\theta,\omega_\theta=\sqrt{1-(\rho')^2}/\rho,\omega'_\theta=\gamma(\omega_\xi-\omega_\theta)\\&\rho''/\rho=-\omega_\xi\omega_\theta,\gamma=\rho'/\rho,\xi=s/a,(\quad)'=d(\quad)/d\xi\end{aligned}\right\}\tag{1}$$

where r is the distance from the axis, s is the meridional distance measured from a boundary along the middle surface and a is the reference length.

Adding the inertia terms to the equilibrium equations in Sanders' theory for thin shells[8] and eliminating the transverse shear forces Q_ξ and Q_θ from these, where the rotatory inertia terms are omitted, the following equations of motion are obtained:

$$\left.\begin{aligned}&a\left[\frac{\partial}{\partial\xi}(\rho\Delta N_\xi)+\frac{\partial}{\partial\theta}(\Delta\bar N_{\xi\theta})-\rho'\Delta N_\theta\right]\\&+\omega_\xi\left[\frac{\partial}{\partial\xi}(\rho\Delta M_\xi)+\frac{\partial}{\partial\theta}(\Delta\bar M_{\xi\theta})-\rho'\Delta M_\theta\right]\\&+\frac{1}{2}(\omega_\xi-\omega_\theta)\frac{\partial}{\partial\theta}(\Delta\bar M_{\xi\theta})\\&+\rho a^2\left[\Delta P_\xi-\rho_0 h\frac{\partial^2}{\partial t^2}(\Delta U_\xi)\right]=0\\&a\left[\frac{\partial}{\partial\theta}(\Delta N_\theta)+\frac{\partial}{\partial\xi}(\rho\Delta\bar N_{\xi\theta})+\rho'\Delta\bar N_{\xi\theta}\right]\\&+\omega_\theta\left[\frac{\partial}{\partial\theta}(\Delta M_\theta)+\frac{\partial}{\partial\xi}(\rho\Delta\bar M_{\xi\theta})+\rho'\Delta\bar M_{\xi\theta}\right]\\&+\frac{1}{2}\rho\frac{\partial}{\partial\xi}[(\omega_\theta-\omega_\xi)\Delta\bar M_{\xi\theta}]\\&+\rho a^2\left[\Delta P_\theta-\rho_0 h\frac{\partial^2}{\partial t^2}(\Delta U_\theta)\right]=0\\&\frac{\partial}{\partial\xi}\left[\frac{\partial}{\partial\xi}(\rho\Delta M_\xi)+\frac{\partial}{\partial\theta}(\Delta\bar M_{\xi\theta})-\rho'\Delta M_\theta\right]+\frac{1}{\rho}\frac{\partial}{\partial\theta}\\&\left[\frac{\partial}{\partial\theta}(\Delta M_\theta)+\frac{\partial}{\partial\xi}(\rho\Delta\bar M_{\xi\theta})+\rho'\Delta\bar M_{\xi\theta}\right]-a\rho(\omega_\xi\Delta N_\xi\\&+\omega_\theta\Delta N_\theta)+\rho a^2\left[\Delta P_\zeta-\rho_0 h\frac{\partial^2}{\partial t^2}(\Delta W)\right]=0\end{aligned}\right\}\tag{2}$$

Here the notations h, t and ρ_0 in the inertia terms are the thickness of the shell, the time and the mass density, respectively, and the modified stress resultant $\bar N_{\xi\theta}$ and the modified stress couple $\bar M_{\xi\theta}$ are[8]:

$$\left.\begin{aligned}\Delta\bar N_{\xi\theta}&=(\Delta N_{\xi\theta}+\Delta N_{\theta\xi})/2+[(1/R_\theta)-(1/R_S)]\\&\quad\times(\Delta M_{\xi\theta}-\Delta M_{\theta\xi})/4\\\Delta\bar M_{\xi\theta}&=(\Delta M_{\xi\theta}+\Delta M_{\theta\xi})/2\end{aligned}\right\}\tag{3}$$

The other variables are shown in Fig. 1.

On the boundary, the effective membrane force $\hat N_{\xi\theta}$ and the effective transverse shear force $\hat Q_\xi$ per unit length are defined as follows[8]:

$$\left.\begin{aligned}\Delta\hat N_{\xi\theta}&=\Delta\bar N_{\xi\theta}+\frac{1}{2}\left(\frac{3}{R_\theta}-\frac{1}{R_s}\right)\Delta\bar M_{\xi\theta}\\\Delta\hat Q_\xi&=\frac{1}{a\rho}\left[\frac{\partial}{\partial\xi}(\rho\Delta M_\xi)+2\frac{\partial}{\partial\theta}(\Delta\bar M_{\xi\theta})-\rho'\Delta M_\theta\right]\end{aligned}\right\}\tag{4}$$

The strains of the middle surface are given by[8]:

$$\left.\begin{aligned}\Delta\varepsilon_{\xi m}&=\frac{1}{a}\left[\frac{\partial}{\partial\xi}(\Delta U_\xi)+\omega_\xi\Delta W\right],\\\Delta\varepsilon_{\theta m}&=\frac{1}{a}\left[\frac{1}{\rho}\frac{\partial}{\partial\theta}(\Delta U_\theta)+\gamma\Delta U_\xi+\omega_\theta\Delta W\right]\\\Delta\varepsilon_{\xi\theta m}&=\frac{1}{2a}\left[\frac{1}{\rho}\frac{\partial}{\partial\theta}(\Delta U_\xi)+\frac{\partial}{\partial\xi}(\Delta U_\theta)-\gamma\Delta U_\theta\right]\end{aligned}\right\}\tag{5}$$

where $\varepsilon_{\xi\theta m}$ is half the usual engineering shear strain.

The relations between the bending distortions χ_ξ, χ_θ, $\chi_{\xi\theta}$ and the rotations Φ_ξ, Φ_θ are as follows[8]:

$$\left.\begin{aligned}&\Delta\chi_\xi=\frac{1}{a}\frac{\partial}{\partial\xi}(\Delta\Phi_\xi),\ \Delta\chi_\theta=\frac{1}{a}\left[\frac{1}{\rho}\frac{\partial}{\partial\theta}(\Delta\Phi_\theta)+\gamma(\Delta\Phi_\xi)\right]\\&\Delta\chi_{\xi\theta}=\frac{1}{2a}\left[\frac{1}{\rho}\frac{\partial}{\partial\theta}(\Delta\Phi_\xi)+\frac{\partial}{\partial\xi}(\Delta\Phi_\theta)-\gamma(\Delta\Phi_\theta)+\frac{1}{2a}(\omega_\xi\right.\\&\left.-\omega_\theta)\left\{\frac{1}{\rho}\frac{\partial}{\partial\theta}(\Delta U_\xi)-\frac{\partial}{\partial\xi}(\Delta U_\theta)-\gamma\Delta U_\theta\right\}\right]\end{aligned}\right\}\tag{6}$$

where

$$\left.\begin{aligned}\Delta\Phi_\xi&=\frac{1}{a}\left[-\frac{\partial}{\partial\xi}(\Delta W)+\omega_\xi\Delta U_\xi\right]\\\Delta\Phi_\theta&=\frac{1}{a}\left[-\frac{1}{\rho}\frac{\partial}{\partial\theta}(\Delta W)+\omega_\theta\Delta U_\theta\right]\end{aligned}\right\}\tag{7}$$

Under the Kirchhoff-Love hypothesis and the neglect of the small quantities ζ/R_s and ζ/R_θ in comparison with unity, the strains at the distance ζ from the middle surface are:

$$\{\Delta\varepsilon\}=\{\Delta\varepsilon_m\}+\zeta\{\Delta\chi\}\tag{8}$$

where

$$\{\Delta\varepsilon\}=\{\Delta\varepsilon_\xi,\Delta\varepsilon_\theta,\Delta\varepsilon_{\xi\theta}\}^T,\ \{\Delta\varepsilon_m\}=\{\Delta\varepsilon_{\xi m},\Delta\varepsilon_{\theta m},\Delta\varepsilon_{\xi\theta m}\}^T,$$
$$\{\Delta\chi\}=\{\Delta\chi_\xi,\Delta\chi_\theta,\Delta\chi_{\xi\theta}\}^T\tag{9}$$

and $\{\ \}^T$ represents the transposed matrix.

Now, we shall use the elasto/visco-plastic equations by Perzyna considering the temperature effect for constitutive relations. The visco-plastic strain rates $\dot\varepsilon_{ij}^{vp}$ are as follows:

$$\dot\varepsilon_{ij}^{vp}=\gamma_0(T)<\Psi(F)>S_{ij}J_2^{-1/2}\tag{10}$$

where the dot denotes the partial differentiation with respect to time, ε_{ij}^{vp}, S_{ij}, J_2 and $\gamma_0(T)$ are the visco-plastic strain, the deviatoric stress, the second invar-

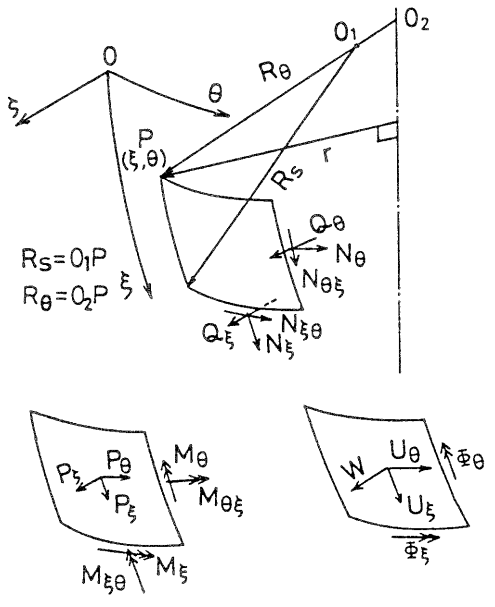

Fig. 1 Coordinates and notations

iant of the deviatoric stress tensor and material constant, respectively. γ_0 is a function of absolute temperature T as well as σ^* in Eq.(12). The symbol $\langle \Psi(F) \rangle$ is defined as follows:

$$F \leqq 0 : \langle \Psi(F) \rangle = 0, \quad F > 0 : \langle \Psi(F) \rangle = \Psi(F) \tag{11}$$

Function F is:

$$F = [\bar{\sigma} - \sigma^*(T)]/\sigma^*(T) \tag{12}$$

where $\bar{\sigma}$ is the equivalent stress ($=\sqrt{3J_2}$) and $\sigma^*(T)$ is the static yielding stress obtained in the usual tension test, which is also a function of the equivalent plastic strain $\bar{\varepsilon}^{vp}$. $F=0$ denotes the von Mises yield surface.

In the present paper when we assume that the total strain increment may be composed of the elastic, the visco-plastic and the thermal parts, the total strain increments in the plane stress state are written as follows:

$$\{\Delta\varepsilon\} = [D]^{-1}\{\Delta\sigma\} + \{\Delta\varepsilon^{vp}\} + \{\Delta\varepsilon^t\} \tag{13}$$

where

$$\{\Delta\sigma\} = \{\Delta\sigma_\xi, \Delta\sigma_\theta, \Delta\sigma_{\xi\theta}\}^T$$

$$\{\Delta\varepsilon^{vp}\} = \{\Delta\varepsilon_\xi^{vp}, \Delta\varepsilon_\theta^{vp}, \Delta\varepsilon_{\xi\theta}^{vp}\}^T$$

$$\{\Delta\varepsilon^t\} = \{\alpha\Delta T_e, \alpha\Delta T_e, 0\}^T$$

$$[D] = \frac{E}{1-\nu^2}\begin{bmatrix} 1 & \nu & 0 \\ \nu & 1 & 0 \\ 0 & 0 & 1-\nu \end{bmatrix}$$

$$\{\Delta\varepsilon^{vp}\} = \{\dot{\varepsilon}^{vp}\}\Delta t = \frac{2}{\sqrt{3}}\gamma_0(T)\left\langle \Psi\left(\frac{\bar{\sigma} - \sigma^*(T)}{\sigma^*(T)}\right)\right\rangle \frac{1}{\bar{\sigma}} \times \begin{bmatrix} 1 & -1/2 & 0 \\ -1/2 & 1 & 0 \\ 0 & 0 & 3/2 \end{bmatrix}\{\sigma\}\Delta t \tag{14}$$

where E, ν and α are Young's modulus, Poisson's ratio, and thermal expansion coefficient, and T_e is the temperature rise from the original temperature T_0 to the present temperature T, namely,

$$T_e(\xi, \theta, \zeta, t) = T(\xi, \theta, \zeta, t) - T_0 \tag{15}$$

Substituting Eq.(8) into Eq.(13) and solving them for stresses, the stresses are:

$$\{\Delta\sigma\} = [D](\{\Delta\varepsilon_m\} + \zeta\{\Delta\chi\}) - \{\Delta\sigma^{vp}\} - \{\Delta\sigma^t\} \tag{16}$$

where

$$\left.\begin{aligned} \{\Delta\sigma^{vp}\} &= \{\Delta\sigma_\xi^{vp}, \Delta\sigma_\theta^{vp}, \Delta\sigma_{\xi\theta}^{vp}\}^T = [D]\{\Delta\varepsilon^{vp}\} \\ \{\Delta\sigma^t\} &= \{\Delta\sigma^t, \Delta\sigma^t, 0\}^T = [D]\{\Delta\varepsilon^t\} = \frac{\alpha E}{1-\nu}\{\Delta T_e, \Delta T_e, 0\}^T \end{aligned}\right\} \tag{17}$$

The membrane forces and the resultant moments per unit length are from Eqs.(16):

$$\left.\begin{aligned} \{\Delta N_\xi, \Delta N_\theta, \Delta\bar{N}_{\xi\theta}\}^T &= h[D]\{\Delta\varepsilon_m\} - \{\Delta N_\xi^{vp}, \Delta N_\theta^{vp}, \Delta\bar{N}_{\xi\theta}^{vp}\}^T - \{\Delta N^t, \Delta N^t, 0\}^T \\ \{\Delta M_\xi, \Delta M_\theta, \Delta\bar{M}_{\xi\theta}\}^T &= \frac{h^3}{12}[D]\{\Delta\chi\} - \{\Delta M_\xi^{vp}, \Delta M_\theta^{vp}, \Delta\bar{M}_{\xi\theta}^{vp}\}^T - \{\Delta M^t, \Delta M^t, 0\}^T \end{aligned}\right\} \tag{18}$$

In Eqs.(18), $(\ )^{vp}$ and $(\ )^t$ denote the apparent internal forces due to visco-plasticity and the internal forces due to temperature rise T_e, respectively, and are given by:

$$\left.\begin{aligned} \{\Delta N_\xi^{vp}, \Delta N_\theta^{vp}, \Delta\bar{N}_{\xi\theta}^{vp}, \Delta N^t\} &= \int_{-h/2}^{h/2}(\Delta\sigma_\xi^{vp}, \Delta\sigma_\theta^{vp}, \Delta\sigma_{\xi\theta}^{vp}, \Delta\sigma^t)d\zeta \\ \{\Delta M_\xi^{vp}, \Delta M_\theta^{vp}, \Delta\bar{M}_{\xi\theta}^{vp}, \Delta M^t\} &= \int_{-h/2}^{h/2}(\Delta\sigma_\xi^{vp}\zeta, \Delta\sigma_\theta^{vp}\zeta, \Delta\sigma_{\xi\theta}^{vp}\zeta, \Delta\sigma^t\zeta)d\zeta \end{aligned}\right\} \tag{19}$$

A complete set of field equations for 36 independent variables: ΔN_ξ, ΔN_θ, $\Delta\bar{N}_{\xi\theta}$, ΔM_ξ, ΔM_θ, $\Delta\bar{M}_{\xi\theta}$, ΔN_ξ^{vp}, ΔN_θ^{vp}, $\Delta\bar{N}_{\xi\theta}^{vp}$, ΔN^t, ΔM_ξ^{vp}, ΔM_θ^{vp}, $\Delta\bar{M}_{\xi\theta}^{vp}$, ΔM^t, $\Delta\sigma_\xi$, $\Delta\sigma_\theta$, $\Delta\sigma_{\xi\theta}$, $\Delta\sigma_\xi^{vp}$, $\Delta\sigma_\theta^{vp}$, $\Delta\sigma_{\xi\theta}^{vp}$, $\Delta\sigma^t$, $\Delta\varepsilon_{\xi m}$, $\Delta\varepsilon_{\theta m}$, $\Delta\varepsilon_{\xi\theta m}$, $\Delta\varepsilon_\xi^{vp}$, $\Delta\varepsilon_\theta^{vp}$, $\Delta\varepsilon_{\xi\theta}^{vp}$, $\Delta\varepsilon^t$, ΔU_ξ, ΔU_θ, ΔW, $\Delta\chi_\xi$, $\Delta\chi_\theta$, $\Delta\chi_{\xi\theta}$, $\Delta\Phi_\xi$, $\Delta\Phi_\theta$ is now given by 36 equations: (2), (5)-(7), (14), (16)-(19).

3. Nondimensional Equations

In order to analyze the problem of the shells under arbitrary unsymmetrical loads, the loads ΔP_ξ, ΔP_θ, ΔP_ζ, ΔT_e and the 32 independent variables, except $\Delta\varepsilon_\xi^{vp}$, $\Delta\varepsilon_\theta^{vp}$, $\Delta\varepsilon_{\xi\theta}^{vp}$, $\Delta\varepsilon^t$, are expanded into Fourier series[11]. Generally, corresponding small letters are adopted as the Fourier coefficients, but the letter s is used for the stress σ.

Substituting these Fourier series into the above 36 equations and appropriately eliminating the variables, the simultaneous differential equations for $\Delta u_\xi^{(n)}$, $\Delta u_\theta^{(n)}$, $\Delta w^{(n)}$ and $\Delta m_\xi^{(n)}$ can be obtained in the matrix form:

$$A_1\boldsymbol{z}'' + A_2\boldsymbol{z}' + A_3\boldsymbol{z} = A_4\boldsymbol{N}' + A_5\boldsymbol{N} + A_6\boldsymbol{M}' + A_7\boldsymbol{M} + A_8\boldsymbol{T}' + A_9\boldsymbol{T} + A_{10}\boldsymbol{P} + A_{11}\ddot{\boldsymbol{z}} \tag{20}$$

where A_1-A_{11} are 4×4 matrices determined from the shell form and materials (A_1-A_3 are the same as in ref.(12)), and $\boldsymbol{z}$, $\boldsymbol{N}$, $\boldsymbol{M}$, $\boldsymbol{T}$, $\boldsymbol{P}$ are as follows:

$$\left.\begin{aligned} \boldsymbol{z} &= \{\Delta u_\xi^{(n)}, \Delta u_\theta^{(n)}, \Delta w^{(n)}, \Delta m_\xi^{(n)}\}^T, \\ \boldsymbol{N} &= \{\Delta n_\xi^{vp(n)}, \Delta n_\theta^{vp(n)}, \Delta\bar{n}_{\xi\theta}^{vp(n)}, 0\}^T \\ \boldsymbol{M} &= \{\Delta m_\xi^{vp(n)}, \Delta m_\theta^{vp(n)}, \Delta\bar{m}_{\xi\theta}^{vp(n)}, 0\}^T, \\ \boldsymbol{T} &= \{\Delta n^t, \Delta m^t, 0, 0\}^T \\ \boldsymbol{P} &= \{\Delta p_\xi^{(n)}, \Delta p_\theta^{(n)}, \Delta p_\zeta^{(n)}, 0\}^T, \qquad ' = d/d\xi \end{aligned}\right\} \tag{21}$$

The increments of internal forces related to the visco-plasticity and the temperature rise in Eqs.(20) and (21) become the following by use of Eqs.(17) and (19):

$$\left.\begin{aligned} \sigma_0\sum_{n=0}^{\infty}\{\Delta n_\xi^{vp}, \Delta m_\xi^{vp}\}\cos n\theta &= \frac{E}{h}\frac{1}{1-\nu^2} \times \int_{-h/2}^{h/2}\left\{1, \frac{a\zeta}{h^2}\right\}(\Delta\varepsilon_\xi^{vp} + \nu\Delta\varepsilon_\theta^{vp})d\zeta \\ \sigma_0\sum_{n=0}^{\infty}\{\Delta n_\theta^{vp}, \Delta m_\theta^{vp}\}\cos n\theta &= \frac{E}{h}\frac{1}{1-\nu^2} \times \int_{-h/2}^{h/2}\left\{1, \frac{a\zeta}{h^2}\right\}(\Delta\varepsilon_\theta^{vp} + \nu\Delta\varepsilon_\xi^{vp})d\zeta \\ \sigma_0\sum_{n=1}^{\infty}\{\Delta\bar{n}_{\xi\theta}^{vp}, \Delta\bar{m}_{\xi\theta}^{vp}\}\sin n\theta &= \frac{E}{h}\frac{1}{1+\nu} \end{aligned}\right\} \tag{22}$$

$$\times\int_{-h/2}^{h/2}\left\{1,\frac{a\zeta}{h^2}\right\}\Delta\varepsilon_{\xi\theta}^{vp}d\zeta$$

$$\{\Delta n^t,\Delta m^t\}=\frac{1}{1-\nu}\frac{1}{h}\int_{-h/2}^{h/2}\left\{1,\frac{a}{h^2}\zeta\right\}\Delta t_e d\zeta$$

$$\sigma_0\sum_{n=0}^{\infty}\{\Delta s_\xi^{vp},\Delta s_\theta^{vp}\}\cos n\theta=\frac{E}{1-\nu^2}\times\{\Delta\varepsilon_\xi^{vp}+\nu\Delta\varepsilon_\theta^{vp},\ \Delta\varepsilon_\theta^{vp}+\nu\Delta\varepsilon_\xi^{vp}\}$$

$$\sigma_0\sum_{n=1}^{\infty}\Delta s_{\xi\theta}^{vp}\sin n\theta=\frac{E}{1+\nu}\Delta\varepsilon_{\xi\theta}^{vp} \qquad (23)$$

The visco-plastic strain increments on the right-hand sides of the equations can be related to the stresses by Eq.(14), and Simpson's 1/3 rule is used for the calculation of integration.

4. Numerical Method

A finite difference method is employed in order to obtain the solution. The usual central difference formulas are used for every mesh point except the discontinuity points and the boundary points of the shell. For the discontinuity points and the boundary points, forward and backward difference equations are employed[11]. The second derivative with respect to time in the inertia terms in Eq.(20) is treated with the backward difference formula proposed by Houbolt[10].

Applying these difference formulas to the fundamental equations (20), the boundary conditions and the continuity equations, the simultaneous equations with respect to $z_{i,j}$(z at any point and at any time) can be obtained. The solutions at any time are obtained by integration of the incremental values at each calculating stage.

5. Numerical Example

As numerical examples, simply supported cylindrical shells made of mild steel are treated and the following two cases are analyzed.

5.1 Example 1 (Nonuniformly heated shell subjected to impulsive internal pressure)

The nonuniformly heated cylindrical shell (Fig. 2) under a semi-sinusoidal internal pressure with respect to time, as shown in Fig. 3(a), is analyzed. The temperature with uniform distribution along the axis and cosine distribution around the half circumference is considered. Two kinds of shells (l=200, 600 mm) are treated and the same loads are applied. Each parameter of temperature and internal pressure in Figs. 2 and 3(a) is as follows:

$$T_0=25°C,\ T_1=75°C,\ P_0=10\ \text{MPa},\ t_0=0.2\ \text{ms} \qquad (24)$$

The geometrical parameters of these shells are:

$$a=l,\ \xi=s/l,\ \rho=1,\ 1/3,\ \rho'=0,\ \gamma=0$$
$$\omega_\theta=1,\ 3,\ \omega_\xi=\omega'_\xi=0 \qquad (25)$$

The increment $\Delta\xi$ in the nondimensional variable ξ is:

$$\Delta\xi=1/2(N-1) \qquad (26)$$

where N is the meridional mesh point number.

Boundary conditions at the points A(i=1) and B(i=N) are,

$$\text{Point A}: \Delta U_\xi=\Delta\hat{N}_{\xi\theta}=\Delta\hat{Q}_\xi=\Delta\Phi_\xi=0$$
$$\text{Point B}: \Delta U_\theta=\Delta W=\Delta M_\xi=0,\ \Delta N_\xi=\Delta P_\zeta\cdot R/2 \qquad (27)$$

The material constants employed in the calculation are as follows[9]:

$$E=189.5\ \text{GPa},\ \nu=0.3,\ \alpha=11.7\times10^{-6}\ °C^{-1},$$
$$\rho_0=7.78\ \text{g/cm}^3$$
$$\sigma^*(T)=207\exp\{0.45(288/T-1)\}\text{MPa},$$
$$\gamma_0(T)=30.12[1+2.6\{(220-T)/273\}^2]\ \text{s}^{-1}$$
$$\Psi(F)=[(\bar{\sigma}-\sigma^*(T))/\sigma^*(T)]^5 \qquad (28)$$

By using these material constants, the stress-strain curves at T=15, 100, 200, 300°C are shown in Fig. 4.

The mesh point numbers N are chosen to be N=51 and 101 for short and long shells, respectively. The division number through thickness of the shell and number of terms of Fourier series are selected as 19 and 20, respectively. The increment of time Δt is determined as 1.0×10^{-3} ms. These values are obtained in consideration of convergency of the solutions, capacity of the computer and computing time.

The variations of displacements U_ξ, U_θ and W with time at specific points are plotted in Figs.5 and 6. The displacements U_ξ and W in the high temperature portion are larger than that in the low temperature

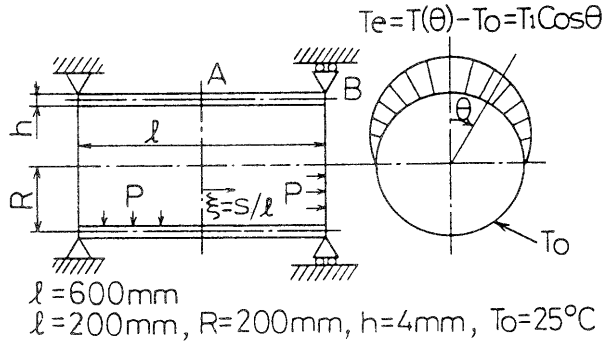

Fig. 2 Cylindrical shell and temperature distribution

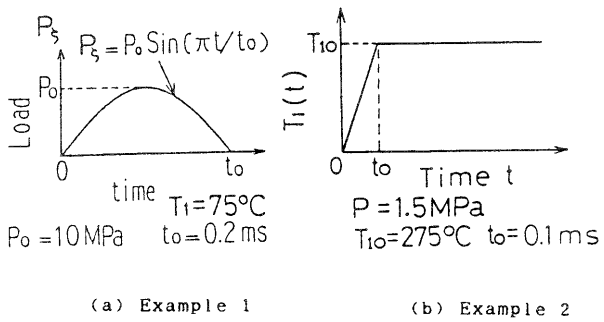

Fig. 3 Impulsive loads (a) Example 1 (b) Example 2

portion. Owing to the application of internal pressure, the above difference becomes large with the lapse of time. It is found from comparisons between long and short shells that the U_ℓ and U_θ of the long shells vary to a great extent with respect to time, but slowly with the lapse of time.

Figure 7 illustrates the variations of membrane force N_ℓ with time at specific points. There is little difference in N_ℓ at these three points but the difference between the solutions of the long and short shells

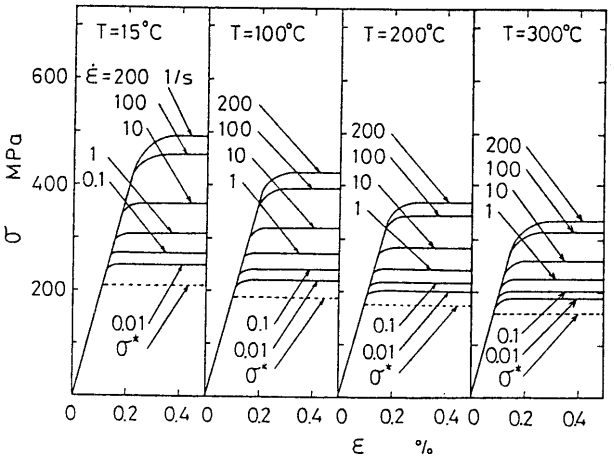

Fig. 4 Stress-strain relations

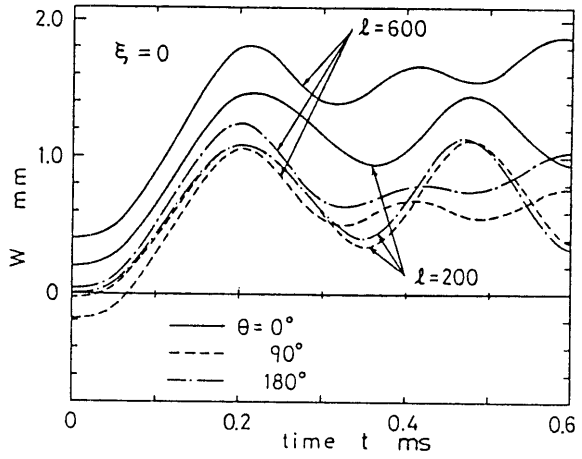

Fig. 5 Variations of W with time

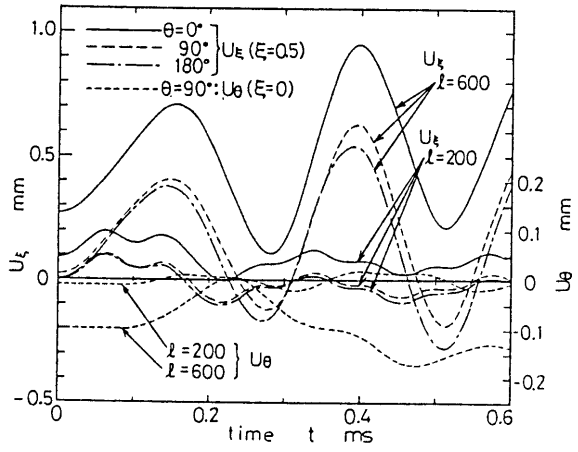

Fig. 6 Variations of U_ℓ and U_θ with time

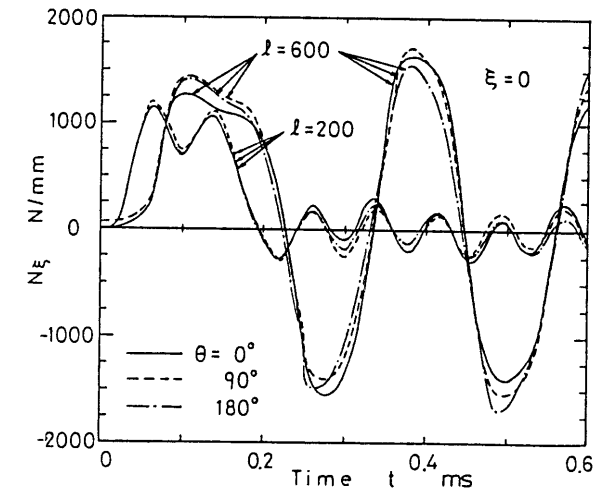

Fig. 7 Variations of N_ℓ with time

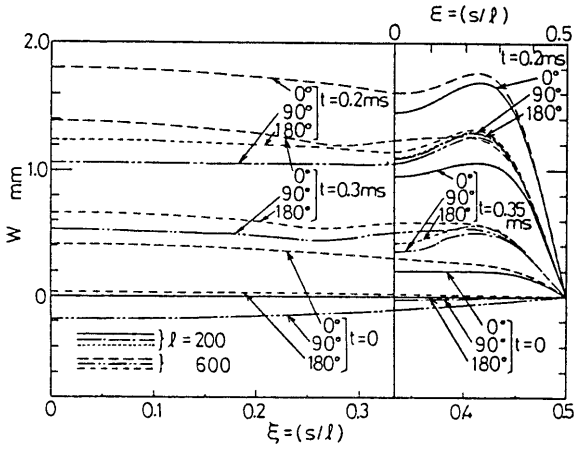

Fig. 8 Meridional distributions of W

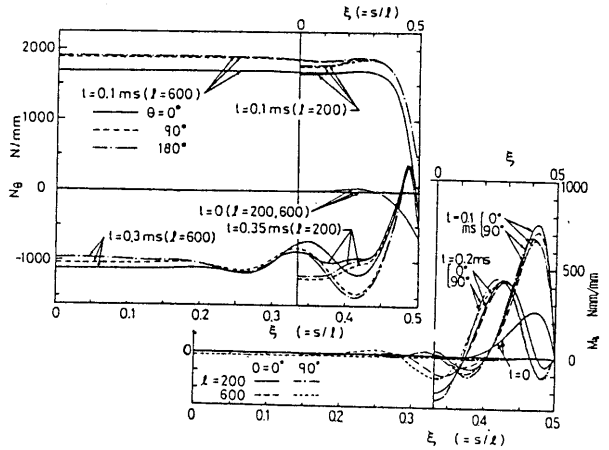

Fig. 9 Meridional distributions of N_θ and M_ℓ

becomes significant after $t=0.2$ ms.

Figures 8 and 9 show the meridional distributions of W and N_θ along $\theta=0$, 90, 180°, and those of M_ξ along $\theta=0$ and 90°. In these figures the meridional coordinates of the long and short shells are taken as proportional to the real length s. It is found from these figures that distributions of these components near the edges in the long shell are similar to the distributions over all the meridian of those in the short shell. In the long shell, W and N_θ are nearly constant along the meridian and the resultant moments are very small except near the edges. Therefore, the membrane stress state occurs except there.

5.2 Example 2 (Internally pressurized shell subjected to impulsive thermal load)

The internally pressurized cylindrical shell under the impulsive thermal load as shown in Figs. 2 and 3 (b) is analyzed. The thermal load with uniform distribution along the axis and cosine distribution around the half circumference is considered. The geometrical parameters, the material constants and the boundary conditions of the shell are the same as in example 1.

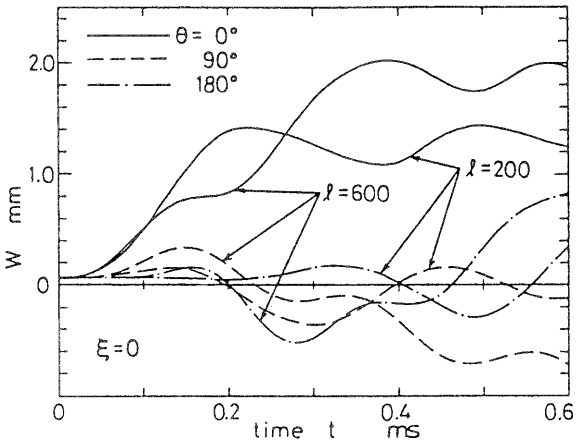

Fig. 10 Variations of W with time

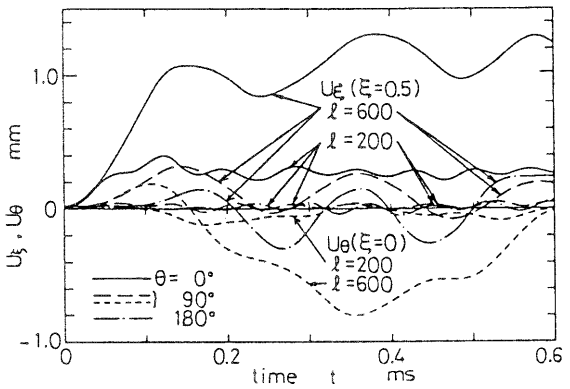

Fig. 11 Variations of U_ξ and U_θ with time

The parameters of internal pressure and thermal load in Figs. 2 and 3(b) are as follows:

$$P=1.5\ \text{MPa},\ T_0=25°\text{C},\ t_0=0.1\ \text{ms},\ T_{10}=275°\text{C} \tag{29}$$

Calculating results are shown in Figs.10-14. Figures 10-12 show the variations of displacements and internal forces at specific points. Owing to the internal pressure the shell deforms slightly in the beginning, and the application of a thermal load induces a large deformation. An especially notable deformation appears in the high temperature portion. It is found via comparison of long and short shells that the displacements and internal forces of the long shells vary a great deal with respect to time, but they respond later and vary more slowly with the lapse of time.

Figures 13 and 14 show the meridional distributions of W and N_θ along $\theta=0$, 90, 180°, $\bar{N}_{\xi\theta}$ along $\theta=90°$, and M_ξ along $\theta=0$, 90°. In Fig. 13 the solid line of $t=0$ coincide with the chain line of $t=0.05$ ms. The

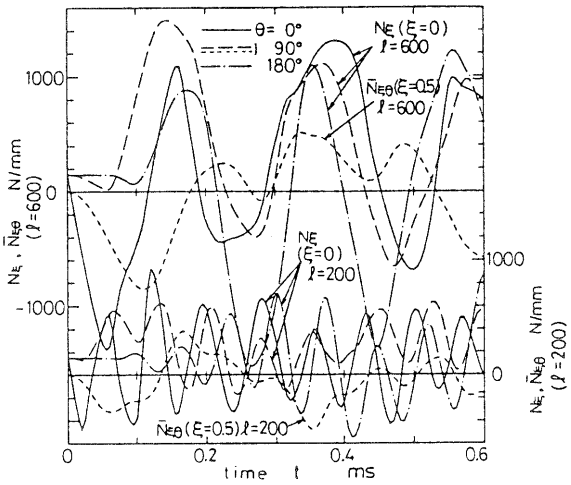

Fig. 12 Variations of N_ξ and $\bar{N}_{\xi\theta}$ with time

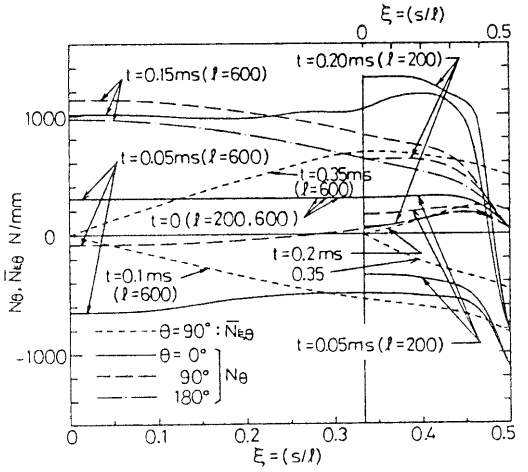

Fig. 13 Meridional distributions of N_θ and $\bar{N}_{\xi\theta}$

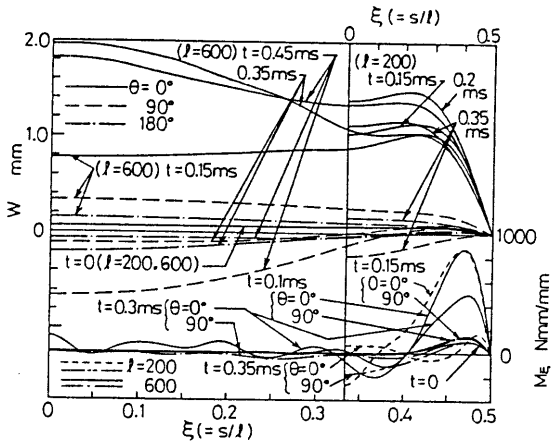

Fig. 14 Meridional distributions of W and M_ξ

distributions of these components near the edges in the long cylindrical shell are similar to the distributions over the entire meridian of those in the short shell, except $\bar{N}_{\xi\theta}$. It is seen from comparison of the distributions of W and M_ξ along $\theta=0, 90, 180°$ that the values along $\theta=0°$. where the thermal load is strong, become large.

6. Conclusions

In this paper the authors have described the numerical analysis of the elasto / visco-plastic dynamic response of axisymmetrical thin shells subjected to mechanical and/or thermal loads. The equations of motion and the strain displacement relations have been derived from Sanders' thin shell theory. The constitutive equations by Perzyna considering the temperature effect have been employed. The numerical method selected for this problem is a method using finite difference in both space and time.

As numerical examples, the simply supported cylindrical shells made of mild steel are treated and the following two cases are analyzed : a nonuniformly heated shell subjected to impulsive internal pressure, and an internally pressurized shell subjected to impulsive thermal load. Two kinds of shell length are adopted in each example. From both numerical examples the following has been found :

(1) The shells deform largely in the portion of the application of high temperature.

(2) From comparison with long and short shells, the displacements and internal forces of the long shells vary a great deal, but they respond more later and vary slowly with the lapse of time.

(3) The meridional distributions of displacements and internal forces near the edges in the long cylindrical shells are similar to the distributions over the entire meridian in the short shells.

The numerical calculation for each example requires about 30 minutes in FACOM M-382.

References

(1) Nagarajan, S. and Popov, E. P., Non-Linear Dynamic Analysis of Axisymmetric Shells, Int. J. Numer. Method in Eng., Vol. 9, No. 3 (1975), p. 535.

(2) Takezono, S. and Tao. K., Elasto/Visco-Plastic Dynamic Response of Shells of Revolution, Trans. 4 th Int. Conf. on Struct. Mech. in Reactor Tech., M 7/7(1977), p. 1.

(3) Takezono, S. and Tao, K., Elasto/Visco-Plastic Dynamic Response of General Thin Shells to Blast Loads, Bull. JSME, Vol. 25, No. 203 (1982), p. 728.

(4) Atkatsh, R. S., Bieniek, M. P. and Sandler, I. S., Theory of Viscoplastic Shells for Dynamic Response, Trans. ASME, Ser. E, Vol. 50, No. 1 (1983), p. 131.

(5) Tao, K., Takezono, S. and Uchibori, H., Elasto/Visco-Plastic Dynamic Response of Moderately Thick Shells of Revolution under Consideration of Rotatory Inertia, Proc. Int. Conf. on Computational Eng. Sci., 2,41, ii (1988), p. 1.

(6) Wojewódzki, W., Buckling of Viscoplastic Cylindrical Shells Subjected to Radial Impulse and Temperature, Trans. 2 nd Int. Conf. on Struct. Mech. in Reactor Tech., Vol. V, Part L 6/7 (1973), p. 1.

(7) Wojewódzki, W. and Bukowski, R., Influence of the Yield Function Nonlinearity and Temperature in Dynamic Buckling of Viscoplastic Cylindrical Shells, Trans. ASME, Ser. E, Vol. 51, No. 1 (1984), p. 114.

(8) Sanders, J. L., Jr., An Improved First-Approximation Theory for Thin Shells, NASA Tech. Rep., R-24(1959), p. 1.

(9) Perzyna, P., Fundamental Problems in Viscoplasticity, Adv. Appl. Mech., Vol. 9 (1966), p. 243, Academic Press.

(10) Houbolt, J. C., A Recurrence Matrix Solution for the Dynamic Response of Elastic Aircraft, J. Aeronaut. Sci., Vol. 17 (1950), p. 540.

(11) Takezono, S. and Uchida, K., Creep Deformations of General Shells of Revolution under Non-Uniform Temperature, Proc. Int. Conf. Eng. Aspect of Creep, Vol. 2 (1980), p. 57.

(12) Budiansky, B. and Radkowski, P. P., Numerical Analysis of Unsymmetrical Bending of Shells of Revolution, AIAA J., Vol. 1, No. 8 (1963), p. 1833.